

Oscillations in feedback driven systems: thermodynamics and noise

Daniele De Martino¹ and Andre C Barato²

¹*Jozef Stefan Institute, Jamova Cesta 39, 1000 Ljubljana, Slovenia*

²*Department of Physics, University of Houston, Houston, Texas 77204, USA*

Oscillations in nonequilibrium noisy systems are important physical phenomena. These oscillations can happen in autonomous biochemical oscillators such as circadian clocks. They can also manifest as subharmonic oscillations in periodically driven systems such as time-crystals. Oscillations in autonomous systems and, to a lesser degree, subharmonic oscillations in periodically driven systems have been both thoroughly investigated, including their relation with thermodynamic cost and noise. We perform a systematic study of oscillations in a third class of nonequilibrium systems: feedback driven systems. In particular, we use the apparatus of stochastic thermodynamics to investigate the role of noise and thermodynamic cost in feedback driven oscillations. For a simple two-state model that displays oscillations, we analyze the relation between precision and dissipation, revealing that oscillations can remain coherent for an indefinite time in a finite system with thermal fluctuations in a limit of diverging thermodynamic cost. We consider oscillations in a more complex system with several degrees of freedom, an Ising model driven by feedback between the magnetization and the external field. This feedback driven system can display subharmonic oscillations similar to the ones observed in time-crystals. We illustrate the second law for feedback driven systems that display oscillations. For the Ising model, the oscillating dissipated heat can be negative. However, when we consider the total entropy that also includes an informational term related to measurements, the oscillating total entropy change is always positive. We also study the finite-size scaling of the dissipated heat, providing evidence for the existence of a first-order phase transition for certain parameter regimes.

PACS numbers: 05.70.Ln, 02.50.Ey

I. INTRODUCTION

Oscillations are a phenomena of paramount importance in physics, biology, chemistry, and economy. They can happen on scales ranging from microscopic to astronomical. They often take place in autonomous nonequilibrium noisy systems that dissipate energy to sustain the oscillations. Prominent examples are autonomous biochemical oscillators, such as systems of interacting molecules that display circadian rhythms driven by the consumption of chemical energy [1, 2].

Fluctuations can fundamentally change the behavior of biochemical oscillations [3–7]. For instance, noise can generate oscillations, in the sense that a biochemical system that has no oscillations in its deterministic description with nonlinear rate equations can display oscillation at the level of a stochastic description that accounts for fluctuations in the finite number of chemical species. Oscillations in such finite noisy systems also have a limited precision. In fact, the relation between the precision of biochemical oscillations and the amount of dissipated energy required to maintain them, analyzed through the lens of stochastic thermodynamics [8], has been the subject of several works [9–15]. Another example of an autonomous nonequilibrium oscillator recently analyzed with the theory of stochastic thermodynamics, is the so-called electron-shuttle [16].

A second class of non-equilibrium noisy systems that display oscillations is a certain phase of periodically driven many body systems known as time-crystal. Time-crystals are systems driven by a time-periodic Hamilto-

nian that display oscillations with a period larger than the period of the drive, so-called subharmonic oscillations. Time-crystals have been studied in closed quantum systems [17–19] and also open systems that dissipate energy [20–23]. Besides displaying spontaneous symmetry breaking of time-reversal symmetry, i.e., the onset of subharmonic oscillations, they also display spatial long range order. The relation between thermodynamics and the precision of subharmonic oscillations in finite stochastic systems has also been investigated with the theory of stochastic thermodynamics in [24].

Hitherto we have mentioned two classes of nonequilibrium systems, autonomous systems driven by a fixed thermodynamic force such as biochemical oscillators and periodically driven systems such as time-crystals. A third class of nonequilibrium systems showing oscillations are feedback driven systems [25], which are of central importance in engineering and technology [26]. These systems are driven out of equilibrium by measurement and feedback, i.e., a change in the Hamiltonian of the system that depends on the measurement outcome. Within stochastic thermodynamics, feedback driven systems have played an important role in elucidating the relation between information and thermodynamics [27–29]. In particular, the total entropy for feedback driven systems includes an informational term related to the increase in entropy generated by the controller that performs the measurements and applies the feedback. An important general feature of deterministic feedback driven systems is that they start to develop oscillations when the controller tries to fix the system onto unstable states, in the presence

of non-linearities [26, 30]. A basic understanding of the thermodynamics of these oscillatory phenomena is still lacking.

In this paper, we provide a systematic analysis of the thermodynamics of temporal oscillations in stochastic feedback driven systems. We start with a simple two-state model that displays oscillations and that can be solved exactly. We then proceed to study a more complex system with several degrees of freedom, a fully interacting Ising model driven by a feedback scheme, which is discrete in time, between the external field and the magnetization. This is a generalization of the model with continuous feedback introduced in [31], which has been shown to display self-oscillations that persist in the thermodynamic limit below the static critical temperature.

The two-state model introduced here provides a paradigmatic, exactly solvable, example of oscillations in feedback driven systems. We show that the number of coherent oscillations, an observable that quantifies the precision of noisy oscillations, can be arbitrarily large in finite feedback driven systems subjected to thermal fluctuations. The size of the system does not impose a fundamental bound on the precision of oscillations in feedback driven systems, in contrast to autonomous systems, for which the number of coherent oscillations is fundamentally bounded by the number of states [11]. We also analyze the relation between thermodynamic cost and precision for this two-state system.

We show that feedback driven systems display a phase similar to time-crystals: the Ising model with discrete feedback we introduce here displays subharmonic oscillations with a period larger than the time-interval between two measurements, which can be taken as the natural period of a feedback driven systems. The oscillations in the magnetization, which persist indefinitely in the thermodynamic limit, take place for temperatures below the critical static temperature.

Concerning the scaling of the rate of entropy production per spin with system size, we show that in the thermodynamic limit this rate is zero above the critical temperature and is larger than zero below the critical temperature. At criticality, the rate of entropy production per spin can either go to zero with a mean field exponent or it can be finite, which correspond to second-order and first-order phase transitions, respectively.

Thermodynamic quantities such as heat and work also oscillate below the critical temperature. We show that while the oscillating dissipated heat can be negative, if we also include the informational contribution to the total entropy change that appears in the second law for feedback driven systems, the total entropy change is positive for all times.

The paper is organized in the following way. In Sec. II we analyze the two-state model. Sec. III is dedicated to the Ising model. We conclude in IV. Appendix A contains a brief introduction to the stochastic thermodynamics of feedback driven systems. The finite-size scaling analysis

of the rate of entropy production for the Ising model with continuous feedback is reported in Appendix B.

II. TWO-STATE MODEL WITH FEEDBACK

A. Definition of the model

We first introduce a simple feedback driven system that displays oscillations. A general definition of thermodynamic quantities in feedback driven systems is provided in Appendix A. The system consists of a single spin with two states $s = \pm 1$. The energy is given by $E_s = -hs$, where h is the external magnetic field. The spin is in contact with a heat bath at temperature T , it flips between these two states due to thermal fluctuations for a time-interval τ . We assume that the dynamics of the system during this time-interval is Markovian. The master equation for the evolution of the probability to be at state $s = 1$ during the n th time-interval reads

$$\frac{d}{dt}p_n(t) = w_1^{h_n}[1 - p_n(t)] - w_2^{h_n}p_n(t), \quad (1)$$

where $w_1^{h_n}$ is the transition rate from state $s = -1$ to state $s = 1$ and $w_2^{h_n}$ is the reversed transition rate. These transition rates fulfill the detailed balance condition

$$\frac{w_2^{h_n}}{w_1^{h_n}} = e^{-2\beta h_n}, \quad (2)$$

where $\beta = 1/(k_B T)$ and k_B is the Boltzmann constant that is set to $k_B = 1$ throughout.

A feedback driven system is also characterized by measurement and feedback. At the end of a time-interval, the state of the system is measured without measurement error. The feedback scheme is such that if the system at the end of the n th time-interval is in the state $s_n = 1$ ($s_n = -1$), then the magnetic field for the next time-interval is set to $h_{n+1} = -h_0$ ($h_{n+1} = h_0$), where $h_0 \geq 0$. We note that the transition rates in Eq. (1) are not fixed quantities but rather they depend on the state of the system in the previous time-interval, i.e., they are random quantities that depend on the particular stochastic trajectory.

B. Oscillatory behavior

This feedback scheme generates oscillations on the average spin orientation at the end of a time-interval as a function of n . In the following we show this property with the exact calculation of the average spin orientation.

We assume that τ is large as compared to the relaxation time to reach the stationary distribution. The probability to be in state $s = 1$ at the end of the n th time-

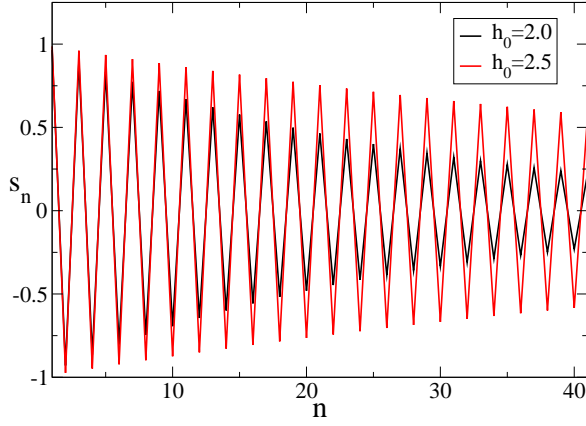


FIG. 1. Oscillations in the two-state model. The inverse temperature is set to $\beta = 1$. The average spin orientation s_n is given in Eq. (7)

interval p_n is then

$$p_n = \frac{e^{\beta h_n}}{2 \cosh(\beta h_n)}. \quad (3)$$

From the feedback rule that the external field for the next time-interval has the opposite sign to the orientation of the spin at the end of the present time-interval, we obtain that the probability p_n follows the recursion relation

$$p_{n+1} = (1 - p_n)p + p_n(1 - p), \quad (4)$$

where

$$p = \frac{e^{\beta h_0}}{2 \cosh(\beta h_0)}. \quad (5)$$

As initial condition we set $h_1 = h_0$ for the first time-interval $n = 1$. The solution of Eq. (4) is given by

$$p_n = \frac{1}{2} [1 - (1 - 2p)^n]. \quad (6)$$

Hence, the average spin orientation $s_n = p_n(+1) + (1 - p_n)(-1)$ reads

$$s_n = (-1)^{n+1} [\tanh(\beta h_0)]^n, \quad (7)$$

where we have used Eq. (5). As shown in Fig. 1, s_n oscillates between positive and negative values with a period $n_{\text{osc}} = 2$ in terms of the integer n . In terms of time such oscillations correspond to a period 2τ , where τ is the time-interval between two measurements. Oscillations in feedback driven systems with a discrete feedback scheme are sub-harmonic, i.e., they have a period of oscillation larger than the natural period of the feedback driven system τ .

C. Relation between precision and work

The amplitude of the oscillations decay exponentially since $\tanh(\beta h_0) \leq 1$. This damping of the oscillations

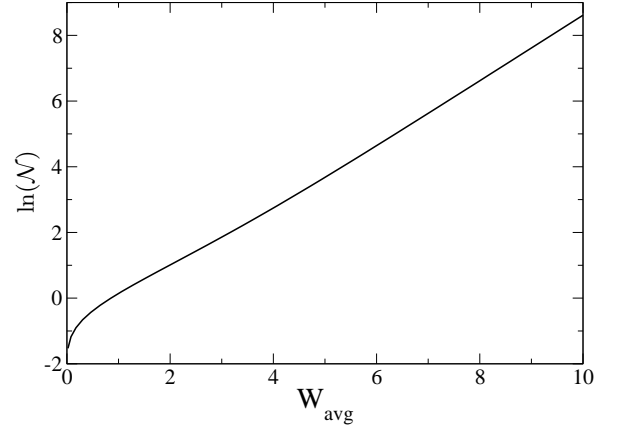


FIG. 2. Parametric plot of $\ln(\mathcal{N})$ versus W_{avg} for the two-state model. The inverse temperature is $\beta = 1$ and the external field is varied from $h_0 = 0.1$ to $h_0 = 5$.

in the average spin orientation is related to noise. If we consider two different stochastic trajectories, after some time they will have different phases due to fluctuations. The number of coherent oscillations that characterizes the precision of the oscillations is defined as the ratio of the decay time and the period of oscillation. If we rewrite Eq. (7) as

$$\begin{aligned} s_n &= \cos(\pi n + \pi) e^{-n[-\ln \tanh(\beta h_0)]} \\ &\equiv \cos(2\pi n/n_{\text{osc}} + \pi) e^{-n/n_{\text{dec}}}, \end{aligned} \quad (8)$$

we obtain the decay time $n_{\text{dec}} = \{-\ln[\tanh(\beta h_0)]\}^{-1}$. The number of coherent oscillations is then

$$\mathcal{N} \equiv \frac{n_{\text{dec}}}{n_{\text{osc}}} = \frac{\{-\ln[\tanh(\beta h_0)]\}^{-1}}{2}. \quad (9)$$

Even though the transition rates during a time-interval fulfill detailed balance, the feedback procedure drives the system out of equilibrium. The average work exerted on the system per time-interval is

$$W_{\text{avg}} = p(2h_0) - (1 - p)(2h_0) = 2h_0 \tanh(\beta h_0). \quad (10)$$

There are two contributions to the work per period. One is the probability to finish a time-interval with the spin and the field pointing in the same direction p multiplied by the energy difference between the two states $2h_0$. The other is the probability to finish a time-interval with the spin and the field pointing in different directions $1 - p$ multiplied by the energy difference between the two states $2h_0$. Unlike the spin orientation, this average work does not oscillate. It is stationary already after the first time-interval.

The relation between precision, as characterized by \mathcal{N} , and energy consumption that is quantified by W_{avg} is analyzed in Fig. 2, where we plot \mathcal{N} as a function of W_{avg} . First, the number of coherent oscillations increases with an increasing energy consumption. Second, at equilibrium ($h_0 = 0$) there are no oscillations. The same property is true for oscillations in autonomous systems such

as biochemical oscillators, since energy dissipation is a general necessary condition for the onset of oscillations. Third, in the limit $\beta h_0 \rightarrow \infty$, both the number of coherent oscillations \mathcal{N} and the work exerted on the system W diverges. This property is in stark contrast with coherent oscillations in autonomous systems. For this case, even in a limit of divergent energy dissipation the number of coherent oscillations is finite and essentially bounded by the number of states [11]. This fundamental difference between oscillations in feedback driven systems and autonomous systems is a main result. The possibility of an indefinite number of coherent oscillations in a finite system in the presence of thermal fluctuations is not exclusive to feedback driven systems. Subharmonic oscillations in periodically driven systems also show this property [24]. A relevant difference between these two cases is that the minimal model for a periodically driven system analyzed in [24] has three states, whereas our minimal model has two states.

D. Informational thermodynamic cost

A distinctive feature of a feedback driven system is that the thermodynamic cost is not only quantified by the work W but also by the mutual information term I , as we report in Appendix A. For this model the information obtained by the measurements is given by

$$I = -p \ln p - (1 - p) \ln(1 - p). \quad (11)$$

Since there is no measurement error, this quantity is just the Shannon entropy of a two-states system at the end of a time-interval, where p is the probability of the lower energy state. This quantity is stationary given that p is the same at the end of all time-intervals. The informational thermodynamic cost I , as compared to the work W_{avg} , has a different relation with the number of coherent oscillations. For $\beta h_0 \rightarrow \infty$, which leads to indefinite oscillations, this cost is minimal, i.e., this limit leads to $p = 1$, which leads to $I = 0$. For $h_0 = 0$, for which there are no oscillations, the mutual information is maximal $I = \ln 2$. As the number of coherent oscillations \mathcal{N} increases, by increasing the parameter h_0 , the informational thermodynamic cost I decreases. This term plays a key role in the entropy balance of more complex feedback driven system as we will show in the following section.

III. ISING MODEL WITH FEEDBACK

A. Model definition

We now consider a fully connected Ising model with N spins and a total of 2^N states. The energy of the system is

$$E_M^h = -JM^2/(2N) - hM, \quad (12)$$

where the magnetization takes the values $M = -N, -N + 2, \dots, N - 2, N$, J is the coupling parameter, and h is the external field. The state of the system is fully characterized by the orientation of all the N spins. However, since the energy of the mean-field model only depends on the magnetization M , the dynamics during a time-interval can be simplified to a random walk on the M space with transition rates fulfilling the detailed balance condition. In particular, we choose the transition rates

$$w_{M \rightarrow M+2}^{h_n} \equiv \frac{\gamma(N - M)e^{\beta[J(m + N^{-1}) + h_n]}}{2 \cosh(\beta[J(m + N^{-1}) + h_n])} \quad (13)$$

and

$$w_{M \rightarrow M-2}^{h_n} \equiv \frac{\gamma(N + M)e^{-\beta[J(m - N^{-1}) + h_n]}}{2 \cosh(\beta[J(m - N^{-1}) + h_n])}, \quad (14)$$

where the subscript n in h_n represents the n th time-interval and γ is a parameter that sets the time-scale of the transition rates. The duration of the time interval is τ . We point out that these transition rates depend on the measurement outcome in the previous time-interval and, therefore, they depend on the particular stochastic trajectory.

The feedback scheme is as follows. At the end of a time-interval, the state of the system is measured with perfect precision and the magnetic field h is changed according to

$$h_{n+1} = h_n - \alpha M_n / N \equiv h_n - \alpha m_n, \quad (15)$$

where α is a constant and M_n is the magnetization at the end of the n th time-interval. There is a similarity between this feedback scheme and the feedback scheme for the two-state model. If the average magnetization is negative then the minimum of the free energy is on the negative side. The feedback is such that the minimum of the free energy is shifted towards the positive side due to the change in the external field. For the opposite case of a positive magnetization, the feedback scheme changes the minimum towards the negative side. Hence, it is expected that this feedback scheme generates oscillatory behavior.

Numerical simulations of this model were performed as follows. We use the Gillespie algorithm [32] to simulate a continuous time random walk with the rates given by Eq. (13) and Eq. (14) for a time-interval τ . At the end of the time-interval the transition rates are updated by a change in the magnetic field given by Eq. (15). The initial condition for our simulations was $h = 0$ for the external field and $M = N$ for the magnetization.

B. Oscillations in the Ising model

This feedback driven Ising model displays oscillations in the magnetization m_n for temperatures below the critical temperature ($T_c = J^{-1}$). As shown in Fig. 3, the

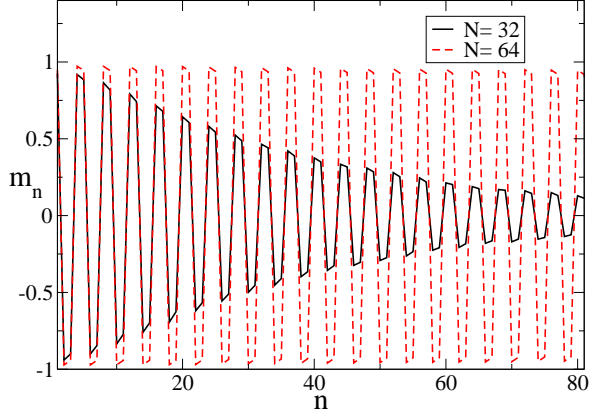


FIG. 3. Oscillations in the feedback driven Ising model. Average magnetization m_n as a function of n . The parameters are set to $\gamma = 1$, $\tau = 100$, $J = 1$, $\beta = 2$, and $\alpha = 0.5$. The period of oscillations, which is the same for both system size for this value of α , is $n_{\text{osc}} = 4$.

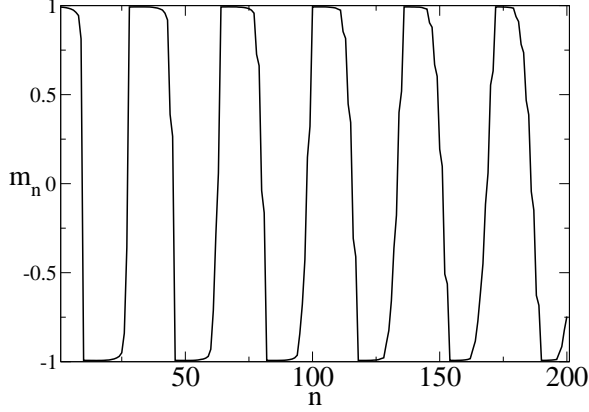


FIG. 4. Effect of the parameter α in the period of oscillation. Average magnetization m_n as a function of n . The parameters are set to $\gamma = 1$, $\tau = 100$, $J = 1$, $\beta = 3$, $\alpha = 0.05$, and $N = 256$. The period of oscillations is estimated to be $n_{\text{osc}} = 36$.

number of coherent oscillations depends on the system size and becomes indefinite in the thermodynamic limit. This feature has been demonstrated analytically for a model with continuous feedback [31].

The oscillatory behavior of the magnetization shown in Fig. 3 is similar to sub-harmonic oscillations in periodically-driven systems with many degrees of freedom, such as time-crystals. An example related to our model is the periodically driven Ising model analyzed in [33], which displays subharmonic oscillations with a period that is two times the natural period of the drive. For the oscillations in our model with the parameters used in Fig 3, the period is four times the time-interval between two measurements.

The period of oscillations has a strong dependence on the parameter α . In Fig. 4 we show that the period of oscillation becomes much larger for $\alpha = 0.05$, as compared to the oscillations shown in Fig. 3 with $\alpha = 0.5$. For this case of a smaller α the period of oscillations is

estimated to be $n_{\text{osc}} = 36$. Besides the parameter α , numerical simulations show that the period depends also on the inverse temperature β .

C. Work and heat for the Ising model

Let us consider a stochastic trajectory of the fully connected Ising model. We denote by M_n the magnetization at the end of the n th time-interval. From Eq. (A3) in Appendix A the total work per spin exerted on the system for a stochastic trajectory with ν time intervals is

$$W = \frac{1}{N} \sum_{n=1}^{\nu-1} (E_{M_n}^{h_{n+1}} - E_{M_n}^{h_n}), \quad (16)$$

where $E_{M_n}^{h_{n+1}}$ is the energy of the system in the beginning of the $(n+1)$ th time-interval and $E_{M_n}^{h_n}$ is the energy of the system at the end of the n th time-interval. We point out that we do not carry out the explicit dependence of the work W on the stochastic trajectory as we do in Appendix A. Furthermore, the quantity W in Appendix A represents the total work whereas here it represents the work per spin, i.e., the work divided by the number of spins N . This quantity is finite in the thermodynamic limit $N \rightarrow \infty$. For all thermodynamic quantities of the Ising model, such as heat and entropy change, we consider the thermodynamic quantity per spin, hence, there is a factor N^{-1} in relation to the generic expressions given in Appendix A. From Eqs. (12) and (15), the work in Eq. (16) becomes

$$\begin{aligned} W &= \sum_{n=1}^{\nu-1} (h^n - h^{n+1}) M_n / N = \sum_{n=1}^{\nu-1} \alpha (M_n)^2 / N^2 \\ &\equiv \sum_{n=1}^{\nu-1} W_n. \end{aligned} \quad (17)$$

The dissipated heat per spin is obtained from Eq. (A5) in Appendix A, together with Eqs. (12) and (15),

$$\begin{aligned} Q &= \sum_{n=1}^{\nu} (E_{M_n}^{h_n} - E_{M_{n-1}}^{h_n}) \\ &= \sum_{n=1}^{\nu} J(M_n^2 - M_{n-1}^2) / (2N^2) + h^n (M_n - M_{n-1}) / N \\ &\equiv \sum_{n=1}^{\nu} Q_n. \end{aligned} \quad (18)$$

The quantity W_n is the work exerted on the system at the end of period n and Q_n is the heat dissipated during the n th time-interval. There is an abuse of notation to represent the averages of M_n , W_n , and Q_n , which are stochastic quantities. In all figures and in all expressions below these symbols represent averages over stochastic trajectories.

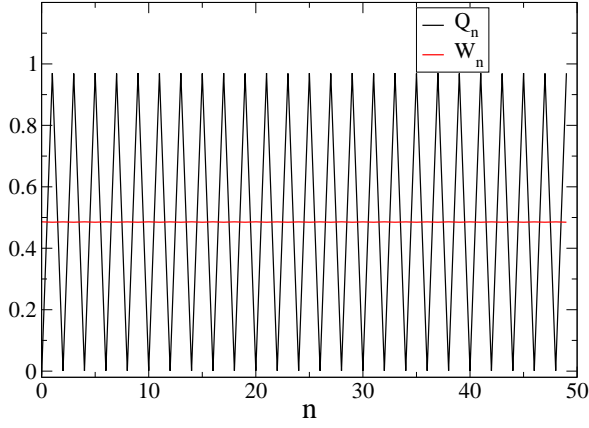


FIG. 5. Oscillations in work and heat. Average work W_n and average heat Q_n as a function of n . The parameters are set to $\gamma = 1$, $\tau = 100$, $J = 1$, $\beta = 3$, $\alpha = 0.5$, and $N = 128$. The amplitude of oscillations for the work W_n , which cannot be seen in this resolution, are much smaller than the amplitude of oscillations for the heat Q_n .

In Fig. 5 we plot heat Q_n and work W_n as a function of n . Both quantities oscillate with a period that is half of the period of oscillations of the magnetization (which is $n_{\text{osc}} = 4$ for this case), since they are both quadratic functions of the variables m and h . The amplitude of the oscillations for the work W_n are much smaller than the amplitude of the oscillations in the heat Q_n .

D. Second law and information

We now analyze the second law for the Ising model with feedback. The average entropy increase of the external environment per spin for the n th time interval is given by $\Delta S_{\text{env}}^n = \beta Q_n$. As shown in Fig. 6, this oscillating quantity can be negative at certain times n . Such negative dissipated heat for a system in contact with a single heat bath would constitute a “violation” of the standard statement of the second law of thermodynamics for systems without feedback. However, for feedback driven systems there is also the informational contribution I_n . The total entropy change per spin for the n th time interval is $\Delta S_{\text{tot}}^n = \Delta S_{\text{env}}^n + I_n \geq 0$, where this second law inequality is discussed in Appendix A. In Fig. 6 we show that while the entropy change of the environment for a certain times n can be negative, when we also account for the informational term the total entropy change ΔS_{tot}^n is positive, as predicted by the second law for feedback driven systems.

The mutual information I_n was calculated in the following way. Since there are no measurement errors the mutual information I_n is just the entropy of the system at the end of the n th time-interval. If we denote a spin configuration with N spins by \mathbf{s} then the mutual

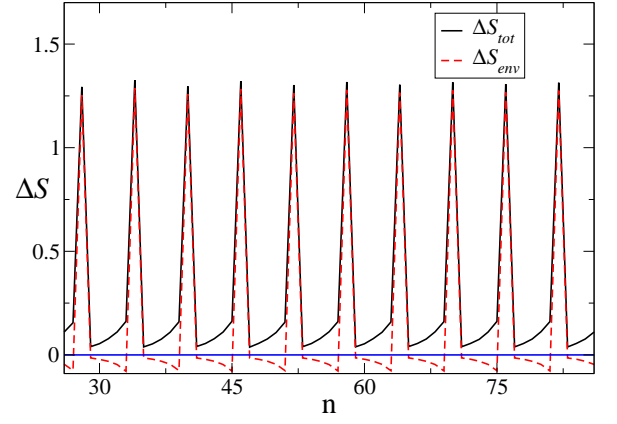


FIG. 6. Second law for the feedback driven Ising model. The entropy change of the environment ΔS_{env}^n , which can be negative, and the total entropy change $\Delta S_{\text{tot}}^n = \Delta S_{\text{env}}^n + I_n$ as functions of n . The parameters are set to $\gamma = 1$, $\tau = 100$, $J = 1$, $\beta = 2$, $\alpha = 0.1$, and $N = 512$.

information per spin is

$$I_n = -\frac{1}{N} \sum_{\mathbf{s}} P_n(\mathbf{s}) \ln[P_n(\mathbf{s})], \quad (19)$$

where $P_n(\mathbf{s})$ is the probability of the spin configuration \mathbf{s} at the end of the n th time interval. The sum in Eq. (19) is over the 2^N spin configurations. For the present mean field model with the Hamiltonian in (12) that only depends on the magnetization M , we have

$$P_n(\mathbf{s}) = P(\mathbf{s}|M)P_n(M) \\ P(\mathbf{s}|M) = \frac{\delta(\sum_i s_i, M)}{\mathcal{C}_{N,M}}, \quad (20)$$

where $P_n(M)$ is the probability of magnetization M at the end of the n th time interval and $P(\mathbf{s}|M)$ is the conditional probability of the spin configuration given the magnetization M , which is uniform over the spin configurations with magnetization M . The number of spins configurations with magnetization M is

$$\mathcal{C}_{N,M} = \frac{N!}{((N-M)/2)!((N+M)/2)!}. \quad (21)$$

From Eq. (19) and Eq. (20) we obtain

$$I_n = -\frac{1}{N} \sum_M P_n(M) \ln(P_n(M)) + \frac{1}{N} \sum_M P_n(M) \ln(\mathcal{C}_{N,M}). \quad (22)$$

The sum in this equation is over the $N+1$ possible values of the magnetization. The mutual information I_n can then be evaluated from a numerical calculation of the probability $P_n(M)$.

E. Scaling of the entropy production

The stationary average change of entropy production per spin and per time-interval is defined as

$$\sigma = \frac{\beta}{\nu} \lim_{\nu \rightarrow \infty} \sum_{n=1}^{\nu} Q_n. \quad (23)$$

We have analyzed numerically the scaling behavior of this quantity of the number of spins N . Above the critical temperature σ tends to a constant value in the thermodynamic limit. Below the critical point σ goes to zero in the thermodynamic limit. At the critical point this quantity shows a scaling behavior that depends on the parameters α and τ . We define the exponent θ as

$$\sigma \sim N^{1-\theta}. \quad (24)$$

In Fig. 7, we plot $N\sigma$ as a function of N for different values of α at fixed τ . For smaller values of α we obtain an exponent compatible with the mean field value of a continuous transition $\theta = 0.5$.

For larger values of α we obtain an exponent compatible with $\theta = 1$. Hence, the entropy production is finite in the thermodynamic limit at the critical point, i.e., for larger values of α there is a first-order phase transition. For intermediate values of α we obtain an effective exponent between 0.5 and 1. However, the effective exponent estimated within a larger N region is larger than the effective exponent for smaller values of N . Hence, for intermediate values of α there is a transient in N which goes beyond the values of N used in our simulations. In Appendix B we characterize analytically the scaling behavior and the phase transition for small α and τ in the model with continuous feedback.

IV. CONCLUSION

We have provided a systematic analysis of oscillations in noisy feedback driven systems. The two-state model introduced here provides arguably the simplest example of such oscillation. Exact calculations with this simple model demonstrate fundamental differences between oscillations in feedback driven systems and the other two kind of oscillators. Importantly, even in a two-state system with thermal fluctuations the oscillations can remain coherent for an arbitrarily long time, in contrast to oscillations in autonomous systems, which can only remain coherent for a finite time that is determined by the number of states of the system [11]. This property of indefinite oscillations in finite systems is also present for subharmonic oscillations in periodically driven systems [24], however, the minimal model in this case was found to have three states, whereas our minimal of a feedback driven oscillator has two states.

The feedback driven fully connected Ising model provides an example of a system with several degrees of free-

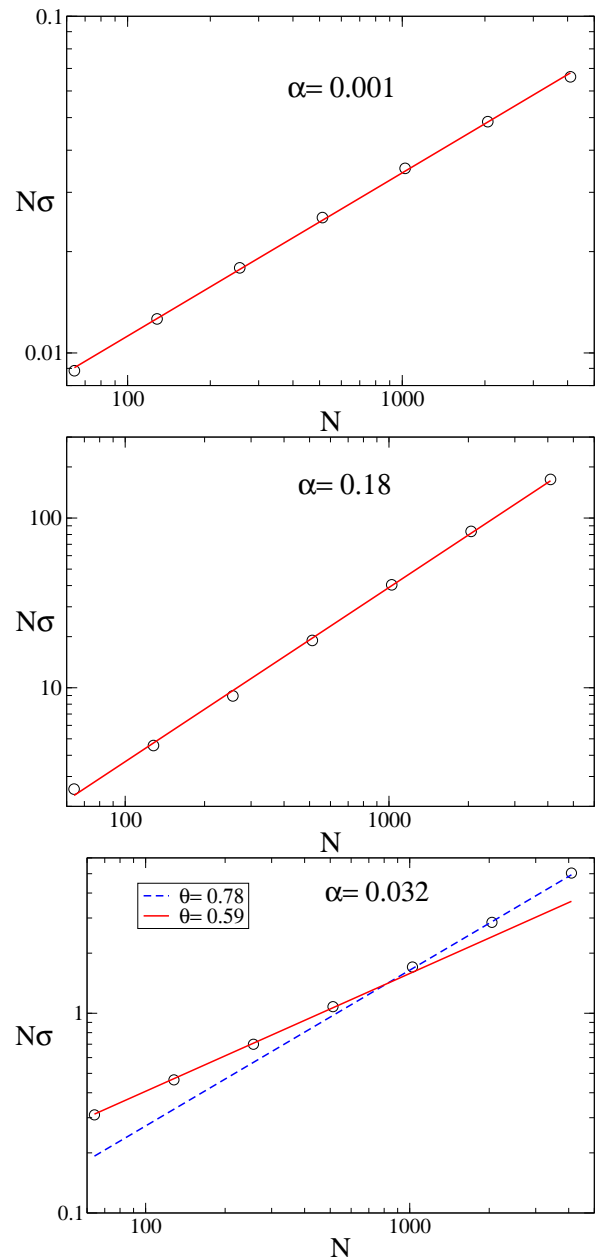


FIG. 7. The entropy production rate σ as a function of the number of spins N at the critical point $\beta = 1$ for different values of α . For the upper panel that is associated with $\alpha = 0.001$, the exponent estimated with the full red line is compatible with $\theta = 0.5$. For the mid panel that is associated with $\alpha = 0.18$, the exponent estimated with the full red line is compatible with $\theta = 1$. For the lower panel that is associated with $\alpha = 0.032$ the effective exponent increases for increasing N . Parameters are set to $\gamma = 1$, $\tau = 100$, and $J = 1$.

dom that has oscillations that become indefinite in the thermodynamic limit, as previously demonstrated in [31] for a model with continuous feedback. We have shown that the model analyzed here with discrete feedback displays subharmonic oscillations in the magnetization similar to the subharmonic oscillations in time-crystals.

The thermodynamic cost of oscillatory feedback driven systems has to be carefully analyzed. We have shown that the oscillatory dissipated heat for the Ising model is negative at certain times, even if the system is in contact with a single heat bath. However, if the informational thermodynamic cost related to measurements is also taken into account the oscillatory total entropy change per time-interval is positive at all times, as predicted by the second law for feedback driven systems. Whereas negative dissipated heat in feedback driven systems is a well known fact, previous studies have not considered the second law for feedback driven systems with oscillators.

A similarity between oscillations in feedback driven systems and in autonomous systems deserves to be mentioned. In both cases, in the deterministic limit, we have instances of self-oscillations [30] that cannot be differentiated at this level of description. However, these feedback driven oscillators and autonomous oscillators are two different classes of oscillators at the stochastic level of description. In particular, they have different limitations concerning the precision of oscillations and the second law of thermodynamics implies different inequalities, with an informational term showing up for feedback driven oscillators.

Concerning future work, it would be interesting to numerically analyze the critical behavior of a two-dimensional Ising model with a feedback scheme similar to the one considered here. In particular, a comparison of such model with time-crystals could lead to an understanding of differences and similarities between oscillatory feedback driven systems and time-crystals, concerning their critical behavior and thermodynamics. From a broader perspective, a theoretical framework for oscillations in stochastic systems and their relation to thermodynamics is emerging. The application of this framework to understand biological oscillators and to produce optimal synthetic oscillators remain key open problems.

Appendix A: Feedback driven systems

1. Definition

In this appendix we define thermodynamic quantities, such as heat, work, and entropy, and discuss the second law for feedback driven systems. A more general theory that includes a fluctuation theorem for feedback driven systems can be found in [28]. Such systems are characterized by Markovian dynamics during time-intervals of duration τ and by measurement and feedback at the end of each time-interval. Mathematically, feedback translates into transition rates for the present time-interval that depend on the measurement outcome at the end of the previous time-interval. Transition rates are then random variables that depend on the particular stochastic trajectory.

We consider a discrete set of states of the system $x = 1, 2, \dots, \Omega$. A stochastic trajectory with total time $\nu\tau$ is denoted by X_ν , where τ is the duration of time-interval. The state of the system and the measurement outcome at the end of the n th time-interval are denoted by x_n and y_n , respectively. The stochastic trajectory $Z_{\nu\tau}$ can be written as

$$Z_\nu = (X_\tau^{\lambda_1}, y_1, X_\tau^{\lambda_2}, y_2, \dots, X_\tau^{\lambda_{\nu-1}}, y_{\nu-1}, X_\tau^{\lambda_\nu}). \quad (\text{A1})$$

The variable λ_n represents the protocol during the n th interval. This protocol λ_n depends on the measurement outcome at the end of the previous time-interval y_{n-1} . Here we restrict to the case of time-independent protocols during the time-interval τ . The stochastic trajectory Z_ν is a sequence of sub-trajectories $X_\tau^{\lambda_n}$ and measurement outcomes y_n . Each sub-trajectory is Markovian and can be written as $X_\tau^{\lambda_n} = (x_i^n, x_1^n, \dots, x_f^n)$, where $x_f^n = x_i^{n+1} = x_n$. For convenience we write this sub-trajectory as discrete in time. The number of elements in the trajectory is the inverse of the time-step multiplied by τ . If we take this time-step to go to zero we recover the continuous-time description.

The measurement outcome y_n is obtained with a pre-assigned conditional probability $P(y_n|x_n)$. Here, we assume that the measurement outcome is independent of the measurement history and only depends on the state of the system x_n . The number of possible states for the measurement outcome can be smaller than Ω , which is the number of states of the system. For example, for the Ising model analyzed in Sec. III, the number of states is $\Omega = 2^N$, whereas the magnetization that is the outcome of the measurement has $N + 1$ possible states.

The transition rate at the n th time-interval from state x to state x' is denoted by $w_{xx'}^{\lambda_n}$. Here, we assume that the transition rates during a time-interval are time-independent and fulfill the detailed balance relation with some energy function $E_x^{\lambda_n}$, i.e.,

$$\frac{w_{xx'}^{\lambda_n}}{w_{x'x}^{\lambda_n}} = e^{\beta(E_x^{\lambda_n} - E_{x'}^{\lambda_n})}. \quad (\text{A2})$$

2. Work and heat

The stochastic work is defined as

$$W[Z_\nu] = \sum_{n=1}^{\nu-1} (E_{x_n}^{n+1} - E_{x_n}^n). \quad (\text{A3})$$

The work exerted on the system is the sum of the changes in energy at the end of a time-interval due to the feedback scheme. As an example, the change in the magnetic field due to feedback for the models analyzed here lead to a change in the energy of the system.

Each jump in the sub-trajectory X_ν^n changes the entropy of the environment, which is connected with the

dissipated heat. In particular, the entropy change of the environment for a jump that changes the state of the system from x to x' is $\Delta S_{\text{env}} = \ln(w_{xx'}/w_{x'x})$. This formula can be seen as a postulate of stochastic thermodynamics [8]. From Eq. A2, we obtain that the entropy change of the external environment associated with the whole sub-trajectory X_ν^n as $\beta(E_{x_{n-1}}^n - E_{x_n}^n)$. The entropy change associated with the trajectory Z_ν is then

$$\Delta S_{\text{env}}[Z_\nu] = \sum_{n=1}^{\nu} \beta(E_{x_{n-1}}^n - E_{x_n}^n). \quad (\text{A4})$$

The dissipated heat $Q[Z_\nu] = \frac{1}{\beta} \Delta S_{\text{env}}[Z_\nu]$, is then given by

$$Q[Z_\nu] = \sum_{n=1}^{\nu} (E_{x_{n-1}}^n - E_{x_n}^n). \quad (\text{A5})$$

From Eq. (A3) and (A5) we obtain the first law of thermodynamics

$$\Delta E[Z_\nu] = W[Z_\nu] - Q[Z_\nu] = E_{x_\nu}^\nu - E_{x_0}^1, \quad (\text{A6})$$

where $\Delta E[Z_\nu]$ is the energy change associated with the trajectory Z_ν .

3. Second law

The total entropy change in a feedback driven system is composed by the change of the entropy of the external environment, the change of the entropy of the system, and change of entropy associated with the information obtained with the measurements. We now consider average entropy changes, instead of the stochastic quantities from the previous subsection. An average here means an average over all possible stochastic trajectories. The average entropy change of the external environment is denoted by ΔS_{env} .

Each measurement at the end of time-interval reduces the uncertainty about the state of the system. In the case of perfect measurements that we consider in the models analyzed here, the uncertainty about the state of the system is completely eliminated. This reduction of uncertainty is accompanied by a reduction of the entropy of the system. Such reduction of entropy must be compensated by an increase of entropy in somewhere else. In other words, a controller that makes measurements and apply feedback according to the measurement outcomes imply an increase of entropy [27].

At the end of the n th time-interval, and an instant before the measurement is take, the average entropy of the system is $H^n(x) \equiv -\sum_x P^n(x) \ln P^n(x)$, where $P^n(x)$ is the probability to be in state x at the end of n th time-interval. After the measurement the entropy is reduced to $H^n(x|y) = -\sum_{x,y} P^n(x,y) \ln P^n(x|y)$. This entropy can be calculated with the knowledge of $P^n(x)$ and $P(y|x)$,

the preassigned conditional probability of the measurement outcome that is independent of n . The joint probability is given by $P^n(x,y) = P^n(x)P(y|x)$. From Bayes' theorem the conditional probability $P^n(x|y)$ is $P^n(x|y) = P^n(x)P(y|x)/P^n(y)$, where $P^n(y) = \sum_x P^n(x,y)$.

The total entropy increase to compensate for the entropy reduction of the system after a measurement from $H^n(x)$ to $H^n(x|y)$ is the mutual information

$$I^n \equiv H^n(x) - H^n(x|y). \quad (\text{A7})$$

This mutual information quantifies the minimal entropy increase that a controller acting on the feedback driven system generates. Mutual information is a standard quantity in information theory and it has the property $I^n \geq 0$ [34]. The action of a controller cannot decrease the total entropy. For the case of the models analyzed here with perfect measurements $H^n(x|y) = 0$, leading to $I^n = H^n(x)$. We point out that for more general feedback driven systems with a feedback scheme that can depend on the measurement history the informational observable that quantifies the entropy change due to the action of the controller is the transfer entropy [28].

The informational change in entropy due to the action of a controller is then

$$\Delta S_{\text{inf}} = \sum_{n=1}^{\nu-1} I^n. \quad (\text{A8})$$

Furthermore, the change in the entropy of the system is

$$\Delta S_{\text{sys}} = H^\nu(x) - H^0(x). \quad (\text{A9})$$

An important difference between ΔS_{sys} and the other two entropy changes is that ΔS_{env} and ΔS_{inf} are both extensive in the number of time intervals ν , whereas ΔS_{sys} does not increase with an increase in ν .

Finally, the second law for feedback driven systems reads

$$\Delta S_{\text{tot}} = \Delta S_{\text{env}} + \Delta S_{\text{inf}} + \Delta S_{\text{sys}} \geq 0. \quad (\text{A10})$$

For this second law we have considered a total time-interval $\nu\tau$. However, this second law is valid for any total time-interval. In particular let us take a total time interval that starts after the measurement at the end of the $(n-1)$ th time-interval and finishes after the measurement at the end of the n th time-interval. Furthermore, we also assume perfect measurements, which reduce the entropy of the system to 0. Hence, $\Delta S_{\text{sys}} = 0$. The second law for such total time-interval then reads

$$\Delta S_{\text{tot}}^n = \Delta S_{\text{env}}^n + I_n \geq 0, \quad (\text{A11})$$

where ΔS_{env}^n is the average entropy change of the environment associated with the n th time-interval. This inequality is the one illustrated in Fig. 6.

Appendix B: Model with continuous feedback

1. Langevin equation and thermodynamic observables

We now consider the Ising system with continuous feedback [31], i.e., a feedback scheme that is applied to the system at every instant. The phenomenological Langevin equation for this Ising model reads

$$\begin{aligned} dm &= \{-m + \tanh[\beta(m + h)]\}dt + bdw \\ dh &= -cmdt \end{aligned} \quad (\text{B1})$$

where the coupling parameter of the Ising model is set to $J = 1$, the magnetization m is a continuous variable between -1 and 1 , w represents the Wiener process, and the noise strength is

$$b = \sqrt{\frac{2}{\beta N}}. \quad (\text{B2})$$

The feedback scheme represented by the second equation in Eq. (B1) is equivalent to the feedback scheme represented by Eq. (15) for the model with discrete feedback in the limit of τ and α very small such that their ratio is finite and given by

$$c = \alpha/\tau. \quad (\text{B3})$$

In the thermodynamic limit, for which the noise term in Eq. (B1) is negligible, the phase transition with spontaneous symmetry breaking in the standard Ising model without feedback is substituted by an Andronov-Hopf bifurcation in this model with feedback, with the onset of oscillations below the critical point [31]. The energy per spin of the Ising model is $u = -\frac{1}{2}m^2 - hm$, the infinitesimal change in energy then reads

$$du = -(m + h)dm - mdh - b^2dt, \quad (\text{B4})$$

where we have used Ito's differentiation rule. The infinitesimal work per spin exerted on the system due to the change in the external field h is

$$dW = -mdh = cm^2dt. \quad (\text{B5})$$

This expression is equivalent to the expression in Eq. (17) for the model with discrete feedback. From the first law, we obtain the infinitesimal dissipated heat per spin as

$$dQ = dW - du \quad (\text{B6})$$

These three differentials are stochastic quantities. The average rate of entropy production is defined as

$$\sigma \equiv \lim_{T \rightarrow \infty} \frac{1}{T} \int^T \langle \frac{dQ}{dt} \rangle dt, \quad (\text{B7})$$

where the brackets denote an average over stochastic trajectories. Note that $\lim_{T \rightarrow \infty} \frac{1}{T} \int^T \langle \frac{du}{dt} \rangle dt = 0$ since the

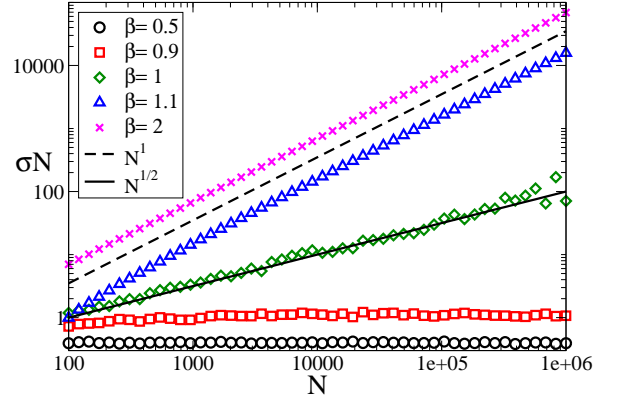


FIG. 8. Scaling of the average rate of entropy production σN in the fully connected Ising model with feedback as a function of the system size N for several temperatures above, at and below the critical point $\beta = 2, 1.1, 1, 0.9, 0.5$ (and $c = 0.1$), from numerical simulations.

energy difference $u(T) - u(0)$ is not extensive in T . Hence, from the first law in Eq. (B6), we obtain

$$\sigma = \lim_{T \rightarrow \infty} \frac{1}{T} \int^T \langle \frac{dW}{dt} \rangle dt = \lim_{T \rightarrow \infty} \frac{1}{T} \int^T c \langle m^2 \rangle dt, \quad (\text{B8})$$

where the second equality follows from Eq. (B5).

2. Analytical calculations for the rate of entropy production

For this model, we derive with an analytical argument, the following scaling law for the average rate of entropy production,

$$\sigma = \begin{cases} \mathcal{O}(1/N) & \beta < 1 \\ \mathcal{O}(1/\sqrt{N}) & \beta = 1 \\ \mathcal{O}(1) & \beta > 1 \end{cases} \quad (\text{B9})$$

This analytical calculation is in agreement with numerical simulations shown in Fig. 8.

First, we consider the case $\beta < 1$. Upon linearizing Eq. (B1) around the stationary point ($m^* = 0, h^* = 0$), we obtain

$$dm = ((\beta - 1)m + \beta h)dt + bdw \quad (\text{B10})$$

$$dh = -cmdt \quad (\text{B11})$$

The stationary value for the square of the magnetization is $\langle m^2 \rangle_s = b^2/2$. Hence, from Eq. (B2) and from Eq. (B7), we obtain that $\sigma = c\beta^{-1}N^{-1}$.

Second, we consider the case $\beta \gtrsim 1$. In the thermodynamic limit the dynamics of the system can be mapped into the equation for the Van der Pol oscillator [31]

$$\ddot{m} + (\beta - 1 - m^2)\dot{m} + \sqrt{c}m = 0. \quad (\text{B12})$$

Performing an expansion in $\beta - 1$, the solution reads

$$\begin{aligned} m(t) &\sim 2\sqrt{\beta - 1} \cos(\sqrt{c}t) + \mathcal{O}(\beta - 1) \\ h(t) &\sim -2\sqrt{c(\beta - 1)} \sin(\sqrt{c}t) + \mathcal{O}(\beta - 1) \end{aligned} \quad (\text{B13})$$

The system is performing harmonic oscillations with the conserved quantity

$$E \equiv m^2 + h^2/c = 2(\beta - 1) \quad (\text{B14})$$

From expression (B7) we obtain that the average rate of entropy production is $\sigma = 2(\beta - 1)$.

Third, we consider the model at the critical point $\beta =$

1. An expansion of $\tanh[\beta(m + h)]$ in Eq. (B1) leads to

$$\begin{aligned} dm &= (h - m^3/3)dt + b dw \\ dh &= -c m dt \end{aligned} \quad (\text{B15})$$

Upon considering the quantity E defined in Eq. (B14), together with Eq. (B15), we obtain the following SDE,

$$dE = (-2/3m^4 + b^2)dt + 2mdw. \quad (\text{B16})$$

Since E is bounded, the time derivative of its average becomes zero in the steady state, which implies the scaling $\langle m^4 \rangle_s = 3b^2/2$. This last equation implies the square root scaling for the average entropy production per spin with the system size N at the critical point.

-
- [1] J. S. van Zon, D. K. Lubensky, P. R. Altena, and P. R. ten Wolde, *Proc. Natl. Acad. Sci. U.S.A.* **104**, 7420 (2007).
 - [2] G. Dong and S. S. Golden, *Curr. Opin. Microbiol.* **11**, 541 (2008).
 - [3] N. Barkai and S. Leibler, *Nature* **403**, 267 (2000).
 - [4] D. Gonze, J. Halloy, and P. Gaspard, *J. Chem. Phys.* **116**, 10997 (2002).
 - [5] L. Meinhold and L. Schimansky-Geier, *Phys. Rev. E* **66**, 050901 (2002).
 - [6] M. Falcke, *Biophys. J.* **84**, 42 (2003).
 - [7] A. J. McKane, J. D. Nagy, T. J. Newman, and M. O. Stefanini, *J. Stat. Phys.* **128**, 165 (2007).
 - [8] U. Seifert, *Rep. Prog. Phys.* **75**, 126001 (2012).
 - [9] H. Qian and M. Qian, *Phys. Rev. Lett.* **84**, 2271 (2000).
 - [10] Y. Cao, H. Wang, Q. Ouyang, and Y. Tu, *Nature Phys.* **11**, 772 (2015).
 - [11] A. C. Barato and U. Seifert, *Phys. Rev. E* **95**, 062409 (2017).
 - [12] B. Nguyen, U. Seifert, and A. C. Barato, *J. Chem. Phys.* **149**, 045101 (2018).
 - [13] C. Fei, Y. Cao, Q. Ouyang, and Y. Tu, *Nat. Commun.* **9**, 1434 (2018).
 - [14] H. Wierenga, P. R. ten Wolde, and N. B. Becker, *Phys. Rev. E* **97**, 042404 (2018).
 - [15] R. Marsland, W. Cui, and J. M. Horowitz, *J. R. Soc. Interface* **16**, 20190098 (2019).
 - [16] C. W. Wächter, P. Strasberg, S. H. L. Klapp, G. Schaller, and C. Jarzynski, *New J. Phys.* **21**, 073009 (2019).
 - [17] K. Sacha, *Phys. Rev. A* **91**, 033617 (2015).
 - [18] V. Khemani, A. Lazarides, R. Moessner, and S. L. Sondhi, *Phys. Rev. Lett.* **116**, 250401 (2016).
 - [19] D. V. Else, B. Bauer, and C. Nayak, *Phys. Rev. Lett.* **117**, 090402 (2016).
 - [20] A. Lazarides and R. Moessner, *Phys. Rev. B* **95**, 195135 (2017).
 - [21] Z. Gong, R. Hamazaki, and M. Ueda, *Phys. Rev. Lett.* **120**, 040404 (2018).
 - [22] R. R. W. Wang, B. Xing, G. G. Carlo, and D. Poletti, *Phys. Rev. E* **97**, 020202 (2018).
 - [23] F. M. Gambetta, F. Carollo, M. Marcuzzi, J. P. Garrahan, and I. Lesanovsky, *Phys. Rev. Lett.* **122**, 015701 (2019).
 - [24] L. Oberreiter, U. Seifert, and A. C. Barato, *Phys. Rev. E* **100**, 012135 (2019).
 - [25] J. Bechhoefer, *Rev. Mod. Phys.* **77**, 783 (2005).
 - [26] K. J. Aström and R. M. Murray, *Feedback systems: an introduction for scientists and engineers* (Princeton university press, Princeton, NJ, 2010).
 - [27] F. J. Cao and M. Feito, *Phys. Rev. E* **79**, 041118 (2009).
 - [28] T. Sagawa and M. Ueda, *Phys. Rev. E* **85**, 021104 (2012).
 - [29] J. M. Parrondo, J. M. Horowitz, and T. Sagawa, *Nature Phys.* **11**, 131 (2015).
 - [30] A. A. Andronov, A. A. Vitt, and S. E. Khaikin, *Theory of Oscillators* (Dover, 1966).
 - [31] D. D. Martino, *J. Phys. A: Math. Gen.* **52**, 045002 (2019).
 - [32] D. T. Gillespie, *J. Phys. Chem.* **81**, 2340 (1977).
 - [33] F. M. Gambetta, F. Carollo, A. Lazarides, J. P. Garrahan, and I. Lesanovsky, arXiv:1905.08826 (2019).
 - [34] T. M. Cover and J. A. Thomas, *Elements of information theory*, (Wiley, New York, 2006), 2nd Ed.